

Tracking Tongue motion from Tagged Magnetic Resonance Images using Harmonic Phase Imaging (HARP-MRI)

Vijay Parthasarathy*, Moriel NessAiver[†], Jerry L. Prince* and Maureen Stone⁺

* Dept. of Electrical and Computer Engineering
Johns Hopkins University, Baltimore, MD 21218.

[†] Department of Diagnostic Radiology
University of Maryland School of Medicine, Baltimore, MD 21201.

⁺ Department of Oral and Craniofacial Biological Sciences
University of Maryland Dental School, Baltimore, MD 21201.

ABSTRACT

Tracking the motion of the tongue, both its surface and its bulk, is important in understanding how the tongue muscles contribute to speech production and control. In order to understand the motion in the interior of the tongue, tagged magnetic resonance imaging (tMRI) has been used. Tags are distinctive features on tMRI images that can be tracked to calculate various indices of motion. The present methods of tracking tags and extracting motion information are manually intensive and time-consuming, however, typically leading only to coarse estimates of the tongue's motion. In this work, we have used harmonic phase magnetic resonance imaging (HARP-MRI) for measuring the motion of the tongue from sinusoidally tagged MR images. HARP-MRI uses Fourier filtering and special processing algorithms to calculate several measures of motion like strains, displacements, and motion tracks of tissue points. From these dense measures of tongue motion, inferences can be drawn on the corresponding muscle activity, which is important to understand speech control and related disorders.

1 INTRODUCTION

The human tongue has a complicated musculature that undergoes local internal deformations which lead to changes in the shape of the tongue surface. These surface shape changes contribute to the production and control of speech. Hence understanding the motion of the tongue both on its surface and its interior is crucial in understanding speech control and nature of speech disorders. Imaging modalities are used both for measuring surface shape changes — e.g. ultrasound, X-ray microbeam, and electropalatography (EPG) [1] — and for measuring internal strain patterns of the tongue — e.g. tagged magnetic resonance imaging (tMRI) [2]

and electromyography (EMG). Among the modalities to quantify internal tongue motion, EMG is an invasive procedure and its data is difficult to collect and interpret [3]. On the other hand tMRI is noninvasive and the images have distinctive features called tags that can be tracked to quantify tissue motion. The measures from tagged magnetic resonance images also require interpretation because it does not distinguish between active muscle contraction and passive tissue compression.

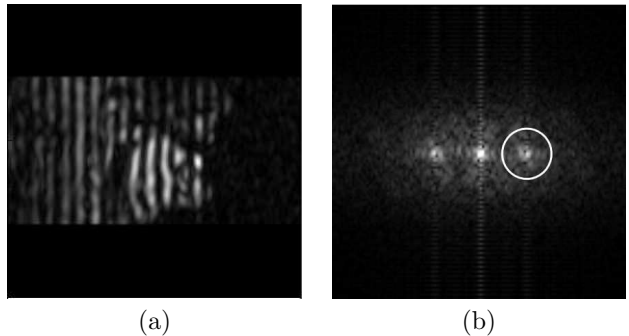


Figure 1: (a) Tagged MR image of midsagittal section of the lower part of the head, and (b) its Fourier magnitude spectrum with HARP bandpass filter.

Fig. 1(a) shows tagged MR image of the midsagittal anatomy of the head. Tags are seen as vertical dark stripes on the image. Tags are temporary features produced by spatially modulating the longitudinal magnetization of the tissue before acquiring image data [4]. Tagged MRI has been used widely to study cardiac deformations and a variety of tag localization algorithms have been developed [5, 6]. In the context of the tongue, tMRI has been used to predict tongue muscle contraction for rest-to-vowel motion, non-speech movements [7, 8, 9, 10] and for 3-D tracking of the tongue [11]. The present methods of analyzing the tagged

images and extracting motion information from it are still manually intensive and time consuming. Moreover the present algorithms lead only to coarse estimates of tongue motion.

In this paper we have used Harmonic Phase magnetic resonance imaging (HARP-MRI) to calculate estimates of motion in the interior of the tongue [12]. HARP-MRI was introduced as a fast automated method for determining myocardial function from sinusoidally tagged MR images. Even though there are differences in the motion of the heart and the tongue, the premise of HARP-MRI that the harmonic phase of a tissue point in a tagged image is directly proportional to the motion of that point, still holds. HARP-MRI uses Fourier filtering and special processing algorithms to calculate different measures of motion. HARP-MRI’s performance has been validated against that of an extensively validated tag analysis method (FINDTAGS) [13, 5]. In order to acquire tagged images with pure sinusoidal tags we acquire images using the CSPAMM approach [14] and combine them using MICSR (Magnitude Image CSPAMM reconstruction) method [15]. We analyze these sinusoidally tagged images using HARP-MRI to get principal strains, motion tracks of tissue points and Lagrangian strains in lines of action of muscle. These measures of motion are dense i.e. not restricted to the points of tag intersections.

The remainder of the paper is organized as follows. Section 2 gives an overview of HARP-MRI and MICSR. Section 3 discusses about the subjects and the speech materials used. We also discuss the methods of calculating the measures of motion used in this paper. Section 4 shows the results of the method and we correlate between the motion measures with muscle activity.

2 BACKGROUND

In this section we give a overview of HARP-MRI and MICSR.

2.1 HARP-MRI

Fig. 1(a) shows a tagged MR image of a human tongue. The tag lines are temporary features that fades gradually until it diminishes in a large fraction of a second. The tag lines, which are straight when they are applied, are bent due to the local deformations in the tongue. The magnitude of the Fourier transform of this image is illustrated in Fig. 1(b). The spectrum consists of a single DC peak and two *harmonic* peaks, which appear because of the spatial modulation caused by the SPAMM tagging [12]. A *harmonic image* can be constructed by band pass filtering one of the harmonic peaks, as shown in Fig. 1(b), and taking its inverse Fourier transform. The resulting complex harmonic image can be expressed as [12]

$$I(\mathbf{y}, t) = D(\mathbf{y}, t)e^{j\phi(\mathbf{y}, t)}, \quad (1)$$

where $\mathbf{y} = [y_1 \ y_2]^T$ is the position vector within an image and t is the time interval after the application of the tags.

The *magnitude image* $D(\mathbf{y}, t)$ is proportional to the transverse magnetization at \mathbf{y} and time t . The *harmonic phase* (HARP) $\phi(\mathbf{y}, t)$ is related to tissue displacement $\mathbf{u}(\mathbf{y}, t)$ as follows

$$\phi(\mathbf{y}, t) = -\boldsymbol{\omega}^T \mathbf{u}(\mathbf{y}, t) + \boldsymbol{\omega}^T \mathbf{y}, \quad (2)$$

where $\boldsymbol{\omega}$ gives the orientation and frequency of the tag pattern in the image plane. The harmonic phase image therefore contains information about the motion of the tissue. In order to completely characterize motion in two dimensions we use both horizontal and vertical tags.

2.2 MICSR

Magnitude Image CSPAMM Reconstruction (MICSR) is a recent method of combining complementary SPAMM (CSPAMM) images using only their magnitude images to reconstruct pure sinusoidal tag patterns — patterns that have no DC peak in their spectrum [16]. The traditional CSPAMM reconstruction [14] method that was designed to eliminate the DC component requires subtraction of two complex datasets which is problematic. The MICSR method bypasses the use of complex datasets by using only magnitude images that have improved contrast, tag persistence. MICSR is also simple to implement and details are given below.

Let ‘A’ represent the series of images obtained using a $[+90^\circ, +90^\circ]$ tagging pulse. Let ‘B’ represent the complementary acquisition, i.e those obtained using $[+90^\circ, -90^\circ]$ tagging pulse. Then the resulting MICSR image is given by

$$I_{\text{MICSR}} = |A|^2 - |B|^2. \quad (3)$$

In order to visualize these MICSR images, NessAiver et. al [16] introduced a trinary display scheme, with gray level values of $[-1, 0, 1]$ (Fig. 2). In this display the tissue will always be black or white while the background (air) will be gray. In Fig. 2 the tags in the two orientations have been multiplied and then thresholded. Even though this display method is not directly related to calculation of motion measures using HARP, it is useful for visualization. In theory, MICSR images are optimized for processing using HARP [15]. Because MICSR produces sinusoidal tags with zero mean, the contamination of the required harmonic spectrum from low frequencies and higher order harmonics is minimized.

3 METHODS

3.1 SUBJECTS AND SPEECH MATERIALS

A 25 year old male, non-native speaker of English demonstrated the application of the method. The sub-

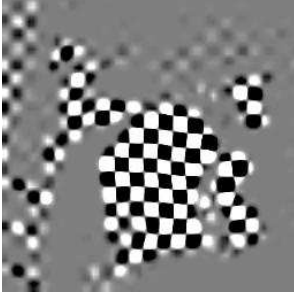


Figure 2: MICSR image.

ject did not have any dental fillings that might interfere with the MRI magnetic field. The speech materials were bisyllables /i/-/a/, /a/-/u/ and /i/-/u/. Since a tagged MR image of an utterance is a combination of repeated utterances, the subject’s ability to repeat the utterances precisely was critical to image quality. Therefore the subject was pre-tested for temporal precision using a metronome that had the same acoustic characteristics as the MRI scanner pulse. Acoustic analysis showed the subject had very little variability. Three sagittal slices were imaged. This paper will present data from the midsagittal slice.

3.2 INSTRUMENTATION AND DATA COLLECTION

Tagged MR images were collected on a 1.5T Marconi Eclipse scanner. The subject lay supine in the MR scanner with the TMJ (temporomandibular joint) phased array coil positioned to image the area from the lower nasal cavity to the upper trachea. Three sagittal slices were collected with a temporal resolution of 66 msec and an interpolated spatial resolution $1.09\text{mm} \times 1.09\text{mm} \times 7\text{mm}$. For each time frame four sets of data were collected: *A*-horizontal, *A*-vertical, *B*-horizontal, and *B*-vertical. The ‘*A*’ sets and ‘*B*’ sets are combined using MICSR method and are shown in Fig. 2. The utterance was repeated twice, one for setup and one for captured utterance. Thus, a tagged image of a slice was composed of 4 repetitions.

3.3 COMPUTING MOTION MEASURES

We have computed three measures of motion: 1) Path lines of tissue points, 2) principle directions and strains, and 3) Lagrangian strain along the action of specific muscles. We now describe how each measure was calculated using HARP-MRI.

1. Path lines of tissue points: A point in the image has two HARP values that can be tracked through a CINE tMRI sequence using *HARP tracking* [12]. Since phase is a material property of the tissue, it can be tracked over time. The result is an estimate of a motion map as shown in Fig. 3. Note that in figs. 3, 4, and 5 we have zoomed into the region around the tongue for better visualization.
2. Lagrangian strain along the line of action of muscle: Given the position of each point using *HARP*

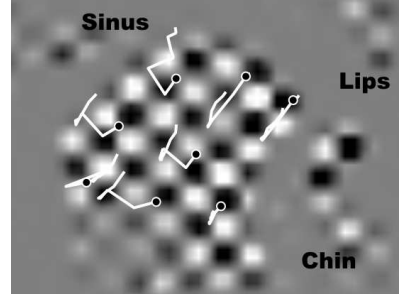


Figure 3: The pathlines of manually selected points (black circles)

Tracking method Lagrangian strains is calculated between any pair of tissue points. Given our aim to infer muscle activity from the tongue using these kinematic measurements, we measured the strains along the directions given in Fig. 4(a).

3. Principal strains: The left Cauchy-Green strain tensor is calculated from the HARP values. Principal strains are the eigenvalues of this tensor. Unit elongation along the principal directions is displayed in Fig. 5 with principal directions superimposed on it. Principal values in most of the region outside the tongue have been masked out because of loss of image intensity in those regions.

4 RESULTS AND DISCUSSION

We demonstrate our results using the bisyllable /i/-/a/. In Fig. 3 we see the motion path of the tissue points in the midsagittal slice. The motion path show the nonlinear motion of the internal tongue tissue points. The black dots represent the position of tissue point in the third time frame. We see that the trajectories in the anterior tongue and the root are approximately linear. The trajectories in the posterior tongue are not linear showing the inhomogeneity of the internal tongue motion.

Fig. 4(a) shows the lines of action for Genioglossus (GG): Posterior (#1) through Anterior (#4), along which Lagrangian strains are calculated. In the motion from /i/ to /a/, the tongue surface lowers and the back moves posteriorly. The strain values in Fig. 4(b) capture the large anterior compression of 30% and the posterior expansion of 50% in the maximal /a/ (time frame 5). The motions of Fig. 3 and the strains of Fig. 4 are consistent with the known surface motions of this gesture and internal tongue compressions seen in previous tMRI data [2, 17]. In addition, the compression in the lines of action of GG is consistent with (though not a proof of) reasonable GG activity in this motion.

Fig. 5 shows principal direction of strains and the elongation along the principal direction for the frame be-

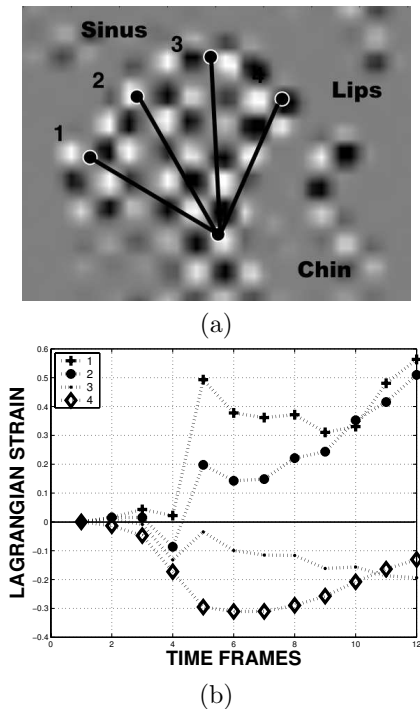


Figure 4: (a) Lines along which Lagrangian strains are calculated, and (b) Lagrangian strain.

fore maximum $/a/$. Substantial compression is seen in the lower front and the tip which is consistent with contraction of GG anterior.

5 CONCLUSION

We have used HARP-MRI to analyze sinusoidally tagged MR images of the tongue. HARP-MRI uses unique spectral properties of tagged image to calculate various motion quantities. In particular, we calculated Lagrangian strains, principal strains, and motion tracks of tissue points. These measures were interpreted to be consistent with internal tongue activity.

ACKNOWLEDGMENTS

This research was supported in part by NIH grant number: R01-DC01758.

REFERENCES

- [1] M. Stone, "Imaging the tongue and vocal tract," *British Journal of Disorders of Communication*, vol. 26, pp. 11–23, 1991.
- [2] M. Stone, E. P. Davis, A. S. Douglas, M. NessAiver, R. Gullapalli, W. S. Levine, and A. Lundberg, "Modelling the motion of the internal tongue from tagged cine-mr images," *Journal of Acoustic Society of America*, vol. 109, no. 6, pp. 2974–2982, 2001.
- [3] A. Perlman, E. Luschei, and C. Dumond, "Electrical activity from the superior pharyngeal constrictor during reflective and nonreflexive tasks," *Journal of Speech and Hearing Research*, vol. 32, pp. 749–754, 1989.
- [4] L. Axel and L. Dougherty, "Heart wall motion: improved method of spatial modulation of magnetization for MR imaging," *Radiology*, vol. 172, pp. 349–350, 1989.

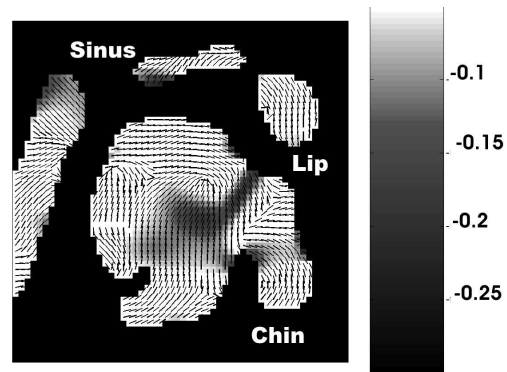


Figure 5: Black lines represent the principal direction of strain and the grayscale represents the elongation along the principal direction.

- [5] M. A. Guttman, J. L. Prince, and E. R. McVeigh, "Tag and contour detection in tagged MR images of the left ventricle," *IEEE Transactions on Medical Imaging*, vol. 13, no. 1, pp. 74–88, Mar. 1994.
- [6] A. A. Young, D. L. Kraitchman, L. Dougherty, and L. Axel, "Tracking and finite element analysis of stripe deformation in magnetic resonance tagging," *IEEE Transactions on Medical Imaging*, vol. 14, no. 3, pp. 413–421, Sept. 1995.
- [7] M. Kumada, M. Niitsu, S. Niimi, and H. Hirose, "A study on the inner structure of the tongue in the production of the 5 Japanese vowels by tagging snapshot MRI," *Annual Bulletin of the Research Institute of Logopedics and Phoniatrics, University of Tokyo*, vol. 26, pp. 1–13, 1992.
- [8] M. Niitsu, M. Kumada, S. Niimi, and Y. Itai, "Tongue movement during phonation: A rapid quantitative visualization using tagging snapshot MRI imaging," *Annual Bulletin of the Research Institute of Logopedics and Phoniatrics, University of Tokyo*, vol. 26, pp. 149–156, 1992.
- [9] V. J. Napadow, Q. Chen, V. J. Wedeen, and R. J. Gilbert, "Biomechanical basis for lingual muscular deformation during swallowing," *American Journal of Physiology*, vol. 277, pp. G695–G701, 1999.
- [10] V. J. Napadow, Q. Chen, V. J. Wedeen, and R. J. Gilbert, "Intramural mechanics of the human tongue in association with physiological deformations," *Journal of Biomechanics*, vol. 322, pp. 1–12, 1999.
- [11] D. Dick, C. Ozturk, A. Douglas, E. McVeigh, and M. Stone, "Three-dimensional tracking of tongue motion using tagged-MRI," in *International Society for Magnetic Resonance in Medicine, 8th Scientific Meeting and Exhibition*, 2000, Denver.
- [12] N. F. Osman and J. L. Prince, "Visualizing myocardial function using HARP MRI," *Phys. Med. Biol.*, vol. 45, no. 6, pp. 1665–1682, June 2000.
- [13] J. Garot, D. A. Bluemke, N. F. Osman, C. E. Rochitte, E. A. Zerhouni, J. L. Prince, and J. A. Lima, "Transmural contractile reserve after reperfused myocardial infarction in dogs," *J. Amer. Coll. Cardiol.*, vol. 36, no. 7, 2000.
- [14] S. E. Fischer, G. C. McKinnon, S. E. Maier, and P. Boesiger, "Improved myocardial tagging contrast," *Mag. Res. Med.*, vol. 30, pp. 191–200, 1993.
- [15] M. NessAiver, V. Parthasarathy, M. Stone, and J. L. Prince, "Magnitude image c-spamm reconstruction (micsr) and harp analysis of tongue motion," in *Proc of ISMRM*, 2003, p. 940.
- [16] M. NessAiver and J. L. Prince, "Magnitude image c-spamm reconstruction (micsr) improves tag contrast and persistence," in *Proc of ESMRMB*, 2002, p. 934.
- [17] M. Stone, D. Dick, E. Davis, A. Douglas, and C. Ozturk, "Modelling the internal tongue using principal strains," in *Proceedings of the 5th Speech Production Seminar, Kloster-Seon*, 2000, pp. 133–136, Germany.